University of Baghdad
College of Engineering
JE
JOURNAL OF ENGINEERING

Journal of Engineering

journal homepage: www.jcoeng.edu.iq

Volume 30 Number 10 October 2024

Exploring the Potential of Nigerian Clay-Based Pozzolans for Enhancing Concrete Performance and Sustainability: A Study on Strength, Hydration, and Durability

Samuel Adesina Adegbemileke *, Sylvester Obinna Osuji , Okiemute Roland Ogirigbo

Department of Civil Engineering, University of Benin, Benin City, Nigeria

ABSTRACT

This study investigated the potential of calcined clays from Nigerian deposits in the production of ternary blends of cement. Clay samples were obtained from three different locations namely: Ikpeshi, Okpilla and Uzebba. The raw clay samples were then calcined at 700°C and 800°C. Chemical and mineralogical compositions were determined for the raw and calcined clay samples using XRF and XRD respectively. The chemical composition confirmed these clays as potential pozzolans with SiO_2, Al_2O_3, and Fe_2O_3 collectively exceeding 70%. XRD analysis identified kaolinite and quartz as major mineral phases in the raw clays, which transformed into metakaolin upon calcination. Compressive strength tests on mortar samples prepared with 50% substitution of Portland cement with the calcined clay and limestone, showed that Ikpeshi clay at 800°C had the best strength performance, with a strength activity index of 0.92 at 28 days, demonstrating superior pozzolanic potential. Strength development was more significant between 7 and 28 days, indicating the pozzolanic reaction's contribution to long-term strength. However, the initial strength at 3 days was lower than the reference cement due to a delayed pozzolanic reaction. XRD analysis of blended pastes revealed typical hydration phases like portlandite, C-S-H, Strätlingite, and ettringite, with the ternary blends showing reduced portlandite content, indicating absorption by the pozzolan's alumina phase. Durability assessments revealed that the ternary blends exhibited improved resistance to water and chloride ion ingress. These findings highlight the effectiveness of Nigerian calcined clays in producing durable and sustainable concrete, supporting their use as supplementary cementitious materials to reduce the environmental impact of concrete production.

Keywords: Calcined clay, Limestone, Supplementary cementitious materials, Portland cement, Nigerian clays.

*Corresponding author
Peer review under the responsibility of University of Baghdad.
https://doi.org/10.31026/j.eng.2024.10.01

Article received: 22/07/2024
Article revised: 12/09/2024
Article accepted: 23/09/2024
Article published: 01/10/2024

1. INTRODUCTION

The increasing global demand for concrete in the 21st century is closely linked to the expansion of the middle class. This trend presents a critical challenge for the concrete industry: to develop and implement systems that enhance the availability of concrete while concurrently mitigating its environmental impact. To effectuate a substantial global transformation, proposed solutions must be scalable, economically viable, and specifically tailored to the requirements of end-users, particularly in developing regions where the majority of demand growth is projected **(Scrivener, 2014)**.

Supplementary cementitious materials **(Juenger et al., 2019)** are soluble siliceous, aluminosiliceous, or calcium aluminosiliceous powders that are used to partially replace clinker in cements or to partially replace Portland cement in concrete mixtures. The primary sources of SCMs are byproducts of industrial processes. These include granulated blast furnace slag, pulverized fly ash, natural pozzolans (such as silica fume and agricultural ashes), artificial pozzolans, and limestone **(Díaz et al., 2017)**. The term "natural pozzolan" refers to a wide variety of materials. While some of these materials are inherently pozzolanic, the majority require processing to develop their pozzolanic properties. They include calcined clay, calcined shale, diatomaceous earth, opaline shales, metakaolin and volcanic materials **(ACI 232.1R, 2012)**. Abundant deposits of such clays are prevalent in equatorial to subtropical regions, which coincidentally align with the geographical locations of many rapidly emerging countries. Given this context, it is highly probable that the demand for cement will continue to escalate in these areas.

The ideal calcination temperature for clay depends on its mineralogical composition and chemical makeup. If the temperature is too low, incomplete dehydroxylation occurs, leaving the structure partially unaltered. Conversely, excessively high temperatures (> 900°C) lead to recrystallization of high-temperature phases and additional sintering, reducing the material's pozzolanic reactivity. Also, The fineness of calcined clay significantly influences its pozzolanic reactivity and performance in cementitious systems. According to studies, a Blaine fineness range of 400-700 m^2/kg is ideal for optimizing the reactivity of calcined clays in concrete applications. However, in this research, the materials were subjected to the same grinding conditions and the effect of fineness on the pozzolanicity was not carried out.

The reaction between the constituent compounds of cement and water is commonly referred to as hydration. During this process, various hydration products form. These include alite, belite, ettringite, calcium monosulfoaluminate, alumina-ferric oxide, monosulfate (AFm), and alumina-ferric oxide trisulfate (AFt). Among these, the primary hydration product is calcium-silicate-hydrate (C-S-H), which typically constitutes 50% to 60% of the hardened cement paste. Lime (calcium hydroxide) makes up approximately 20% to 25%, while ettringite accounts for 15% to 20%. The remaining 5% to 6% consists of capillary voids and entrapped air. Calcium hydroxide, although beneficial for concrete by acting as a buffer with a high pH that protects steel against corrosion, can also be a source of weakness. It is highly soluble and susceptible to attack by acids. Additionally, calcium hydroxide is the most unstable phase in terms of carbonation **(Stark and Wicht, 2000)**. The occurrence of the unreacted lime acts as an activator for the pozzolanic reaction.

Research conducted at the École Polytechnique Fédérale de Lausanne (EPFL) **(Alujas et al., 2015; Avet et al., 2016)** has demonstrated that including approximately 40% kaolinite in an LC3-50 mixture (comprising 50% ground clinker, 30% calcined clay, 15% limestone, and 5% gypsum) yields mechanical properties comparable to those of plain Portland cement

within approximately 7 days. The specific test conditions involved mortar bars with a water-to-cement ratio (w/c) of 0.5 and a sand-to-cement ratio of 3 **(BS EN 196-1, 1995)**.
When evaluating a novel cement formulation, the aspect of durability assumes paramount significance. Hydration of Portland cement produces CH; the CH (Portlandite) reacts with the additional pozzolan to produce calcium silicate hydrates. According to **(Sabir et al., 2001)**, the CH released during the hydration of PC could be harmful to durability and contributes less to strength, thus, the reduction of the released CH by way of reaction with the pozzolan helps to enhance durability and strength. **(Odriozola and Gutiérrez, 2008)** conducted a comparative analysis of various test methods for assessing the chloride permeation resistance of concrete. They found out that, porosity, water absorption, and oxygen permeability tests did not adequately reflect the impact of supplementary cementitious materials or exposure conditions. However, water permeability, capillary water absorption, and depth of water penetration exhibited meaningful correlations with the apparent chloride ion diffusion coefficients of concrete. In contrast, **(Hedayat and Baniasadizade, 2015)** reported that the water absorption test accurately predicts concrete durability against chloride ion ingress. Clay is a complex material and there are no two kaolin exhibiting equal properties. Research into the optimum calcination temperature of the Nigerian kaolinite clay for LC3 applications is lacking. According to **(Rautureau et al., 2017)** kaolin properties are influenced by environmental formation and deposition conditions.
Hence, this research aims to investigate the potential use of clays obtained from Nigeria clay deposits in the production of ternary blends of cement, via assessment of its mechanical and transport properties.

2. MATERIALS AND METHODS

2.1 Materials

2.1.1 Clay

Clay samples were collected from three locations in Edo state, Nigeria: Uzebba (in Owan West Local Government Area), Okpella (in Etsako East Local Government Area), and Ikpeshi (in Akoko-Edo Local Government Area). These areas experience a warm-humid tropical climate characterized by distinct dry and wet seasons. The vegetation in these regions is typical of the Guinea Savannah, featuring shrubs, dispersed trees, and grass savannah. The Uzebba area is situated within the Eastern Dahomey Basin in southwestern Nigeria, where the underlying Upper Cretaceous sedimentary rocks belong to the Araromi Formation. This formation comprises fine to medium-grained fluvial sandstone and gritstone at the base and is covered by shales and siltstones with interbedded marl, limestone and lignite **(Adewumi et al., 2016)**. The region of Okpella and Ikpeshi lies within the Pre-Cambrian Basement Complex of Southwestern Nigeria. Most parts of this region are underlain by the metasediments, referred to as the Igarra Schist Belt **(Ademila et al., 2019)**. The raw clay samples were calcined at temperatures of 700°C and 800°C in a fixed-bed furnace with a heating rate of 10°C/minute and a retention time of 2 hours, to produce calcined clay. Samples of the raw and calcined clay are shown in **Fig. 1**.

(a)

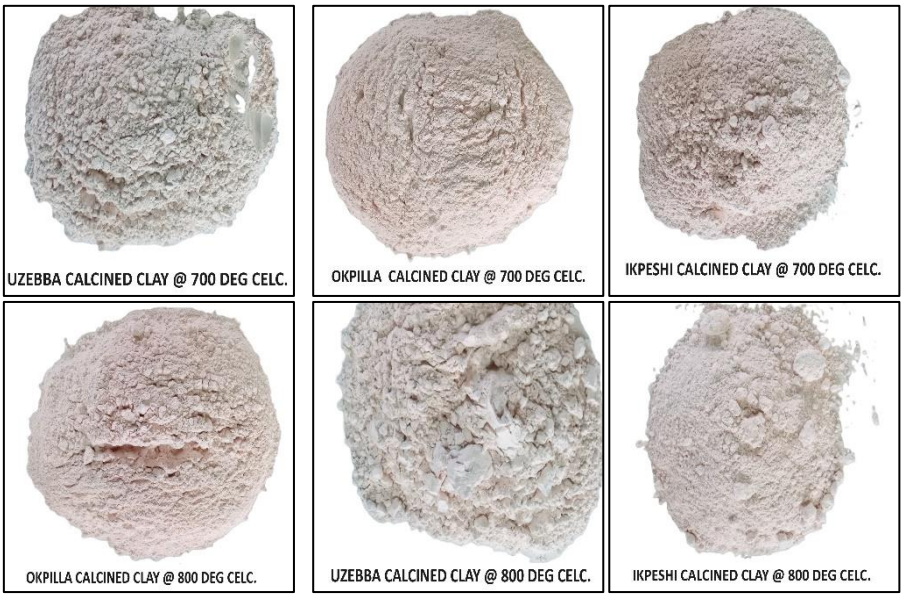

(b)

Figure 1. (a) Raw clay samples (b) Calcined clay samples.

2.1.2 Limestone

The limestone used in the study was obtained as a commercial product from Okpilla.

2.1.3 Portland Cement (PC)

For this study, normal CEM II cement of grade 42.5N was utilized as the reference cement.

The physico-chemical properties of the CEM II cement are presented in **Table 1** alongside the clinker phases present in the cement.

2.1.4 Fine Aggregate

The fine aggregate employed for fabricating test specimens was natural silica sand, which complies with the specifications for graded standard sand **(ASTM C 778, 2002)**. This is a standard sand, predominantly graded to pass a 850-µm (No. 20) sieve and be retained on a 600-µm (No. 30) sieve.

2.1.5 Water

Potable water obtained from the Institute's main supply was employed for the preparation of samples, adhering to standards **(ASTM-C1602/C1602M, 2012)**.

Table 1. Chemical Composition of CEM II cement 42.5N **(Nwokocha and Munachiso, 2022)**

Component	Composition (wt.%)	BS Limits
SiO_3	20.26	17.46-21.59%
Al_2O_3	4.96	3.29-6.14%
Fe_2O_3	3.08	1.21-3.76%
CaO	53.69	58.67-63.90%
MgO	1.06	0.61-3.30%
SO_3	1.53	<3.5
K_2O	0.52	
Na_2O	0.27	
K_2O+Na_2O	0.79	<2.0
C_3S	23.3	50-70%
C_2S	40.67	15-30%
C_3A	7.94	5-10%
C_4AF	9.36	5-15%

2.2 Preparation of Mortar and Paste Samples

Mortar samples were prepared using 1 part of cementitious material and 2.75 parts of sand, with a water/binder ratio of 0.5. The PC-limestone-calcined-clay blends were prepared using 50% of Portland cement, 30% of calcined clay, 15% of limestone and 5% of gypsum (see **Table 2**). The mortar specimens were carefully covered with thin polyethylene sheets and allowed to cure in ambient air conditions for 24 hours. Thereafter, they were demoulded and placed in saturated limewater to cure till the day of testing.

Table 2. Mixture proportioning for LC3 systems.

Sample	Source	Calcination Temp. (^{0}C)	Clinker (% wt. binder)	Calcined clay (% wt. binder)	Limestone (% wt. binder)	Gypsum (% wt. binder)	w/b ratio
OPC	-	-	100.0	0	0	0	0.5
LC3i7	Ikpeshi	700	50.0	30.0	15.0	5.0	0.5
LC3i8		800	50.0	30.0	15.0	5.0	0.5
LC3o7	Okpilla	700	50.0	30.0	15.0	5.0	0.5
LC3o8		800	50.0	30.0	15.0	5.0	0.5
LC3u7	Uzebba	700	50.0	30.0	15.0	5.0	0.5
LC3u8		800	50.0	30.0	15.0	5.0	0.5

Paste samples were prepared using calcined clay and slaked lime in a 40:60 proportion. The calcined clay and slaked lime were placed in a bowl, and dry mixed. Thereafter, water was added to the mixture in a 1:1 water-to-solid ratio. The resulting mixture was stirred thoroughly for one minute with a spoon. Thereafter, the paste was placed into four plastic bottles (each holding about 10ml), and sealed. To avoid carbonation, it is crucial to move fast and effectively during this procedure. Also, the sample tubes were pressed as they were

being filled up so as to help prevent the inclusion of air bubbles, which contain CO_2. In order to promote the hydration reaction over the carbonation reaction, the pastes were then kept in a fog room to cure

2.3 Methods

2.3.1 Chemical Analysis by XRF

The chemical composition of the clays sourced from the three different locations was analysed to assess their suitability as natural pozzolans. The Xenemetrix Genius-IF EDXRF spectrometer was utilized for this analysis. Approximately 5g of pulverized clay sample was filled into each cup, and the analysis was conducted to determine the chemical composition.

2.3.2 Mineralogical Analysis of Raw and Calcined Clay by X-ray Diffraction

X-ray diffraction (XRD) was employed to study the mineralogical composition of the raw and calcined clay samples. Samples were prepared using a compression technique and analyzed on a Rigaku MiniFlex 600 XRD Diffractometer. The settings included a two-theta range from 4° to 75°, using Cu-Kα radiation, with specific parameters for intensity recording and peak identification.

2.3.3 Mortar Strength Test

Compressive strength test was performed on mortar samples at ages of 3, 7 and 28 days. At the day of the test, the mortar samples were brought out from the curing tank and left to dry under air before testing. The cubes were crushed using a Matest compression-testing machine loaded at the rate of 2000N/s. The test was conducted in accordance to the specifications in (**ASTM-C109/109M, 2008).**

2.3.4 XRD Analysis on Ternary Blend Paste

The hydration process and phase changes during hydration were monitored using the Rigaku MiniFlex 600 XRD Diffractometer, with settings consistent with those mentioned earlier.

2.3.5 Transport Properties

2.3.5.1 Sorptivity Test

The sorptivity test was carried out by adopting a similar method used by other researchers **(Güneyisi and Gesoğlu, 2008; Tasdemir, 2003)**. Standard 50 mm mortar cubes were cast from each mixture. After 24 hours, the specimens were demolded and cured in water for 28 days in a water tank. Preconditioning involved oven-drying the specimens at approximately 105°C until a constant mass was achieved. Subsequently, the test specimens were exposed to water on a 50×50 mm plane by placing them in a pan (refer to **Figure 2**). Throughout the experiment, the water level in the pan was maintained approximately 5 mm above the base of the specimens. To ensure unidirectional flow, the lower surfaces of the specimen sides were coated with waterproof material. At predetermined time intervals (1, 4, 9, 16, 25, 36, 49, and 64 minutes), the specimen masses were measured using a scale. The absorbed water

amount was then normalized with respect to the cross-sectional area of the specimens. The sorptivity coefficient (k) was determined using the following expression;

$$k = \frac{Q}{A\sqrt{t}} \quad (1)$$

where,
Q = the amount of water absorbed in cm^3, obtained by dividing the mass of the water absorbed in g, by the density of water (1 g/cm^3)
A = the cross-section of the specimen in contact with water in cm^2
t = time in s
k = sorptivity coefficient of the specimen in $cm/s^{1/2}$.

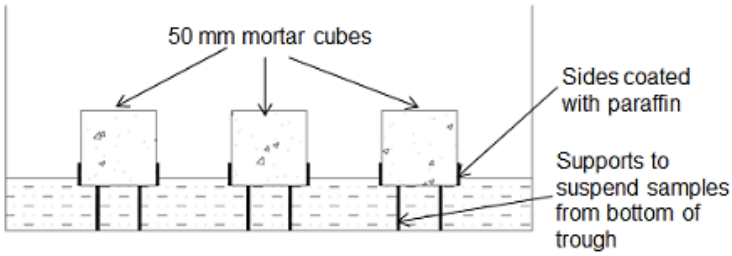

Figure 2. Measurement of water capillary sorption.

Sorptivity coefficient is a measure of the ability of mortar or concrete to absorb water by capillary action. It quantifies the rate at which water is absorbed into the concrete's pore structure under the influence of capillary suction. In simpler terms, sorptivity coefficient tells you how quickly water can penetrate into concrete, which is crucial for understanding its durability, especially in environments where water exposure is a concern **(Balakrishna et al., 2018; Ogirigbo and Black, 2017).** To determine the sorptivity coefficient, the ratio of water absorption (Q) to the exposed cross-sectional area (A) was plotted against the square root of time (t) **(ASTM C1585, 2009)**. The coefficient (k) was then obtained from the slope of the linear relationship between Q/A and t (
Figure 3).

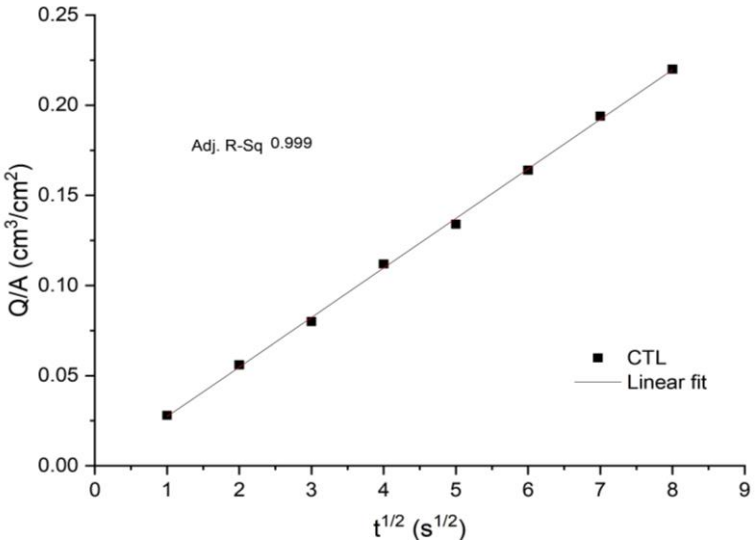

Figure 3. Linear fit for the determination of sorptivity coefficient for a CTL mortar sample cured for 28 days.

2.3.5.2 Depth of Chloride Penetration by Silver Nitrate Calorimetric Technique

The corrosion of steel reinforcement bars in concrete, triggered by the chemical attack of chloride ions (especially in contact with seawater), remains a significant durability challenge for reinforced concrete structures. The diffusion of chloride ions through concrete primarily occurs due to the material's porosity properties **(Loser et al., 2010)** and the specific phase assemblage of the binder material **(Arya et al., 1990; Arya and Xu, 1995)**
The depth of chloride ion penetration was determined by the silver nitrate ($AgNO_3$) spray technique. This technique was used in this study as demonstrated by several researchers **(Güneyisi and Mermerdaş, 2007; Güneyisi et al., 2007; Kim et al., 2007; Luping and Nilsson, 1993; Ogirigbo, 2016)**. After curing for a period of 28 days, the 50 mm cubes were fully immersed in a 3% NaCl solution **(Figure 4)**. The specimens were periodically withdrawn at 14, 28, 56, 90 and 180 days to determine the depths of chloride ion penetration. Afterwards, the withdrawn specimens were split into half and the surfaces were sprayed with a 0.1M silver nitrate ($AgNO_3$) solution. The appearance of a white precipitate (silver chloride, AgCl) indicates the presence of free chloride ions (as described by Equation 2). Conversely, in the absence of free chloride ions, the reaction between portlandite and silver nitrate leads to a brown coloration, signifying the formation of silver hydroxide (AgOH). To assess the depth of free chloride penetration, linear measurements were taken from the specimen's edge to the boundary where the color change occurred.

$$Ag^{+}_{(aq)} + Cl^{-}_{(aq)} \rightarrow AgCl_{(s)} \text{ (white precipitate)} \quad (2)$$

$$Ag^{+}_{(aq)} + OH^{-}_{(aq)} \rightarrow AgOH_{(s)} \text{ (brown precipitate)} \quad (3)$$

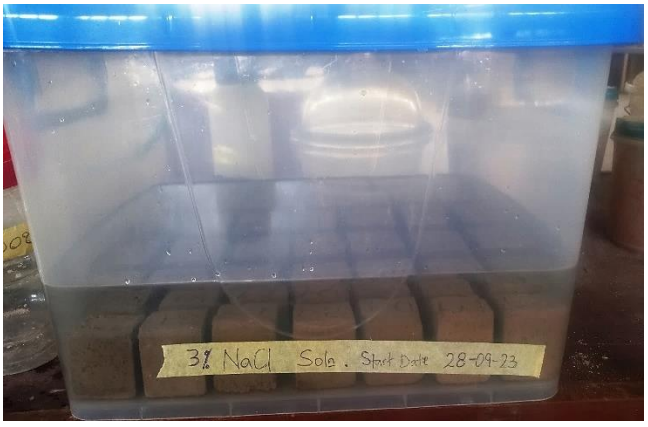

Figure 4. Mortar samples immersed in 3% NaCl solution

3. RESULTS AND DISCUSSION

3.1 Mineralogical and Chemical Compositions of the Raw and Calcined Clays

The result of the bulk chemical analysis of the raw clay and limestone is presented in **Table 3Error! Reference source not found.**. Summation of the components $SiO_2 + Al_2O_3 + Fe_2O_3$ is equal to or greater than seventy percent (70%), indicating that the three clays can be classified as potentially good pozzolans **(ASTM-C-618, 2005)**. The clays from the three sources have high alumina (Al_2O_3) contents varying between 28.89 and 38.24 % and silica

(SiO_2) content ranging from 39.35 to 60.87 %. The Fe_2O_3 content of the samples are between 1.18 and 1.95 % and that of TiO_2 varies between 2.74 and 5.28 %. There was a high CaO content of 24.60 % in the Ikpeshi raw clay. According to the French norm for metakaolin **(NF P 18-513, 2012)**, the LOI value should not be more than 4 %. Determination of the LOI for the clay materials from the three locations revealed low values of 1.03, 2.05 and 2.29 % for the Ikpeshi, Okpilla and Uzebba clays, respectively. A correlation between the alumina content and the LOI was observed. As the LOI value increased, there was a corresponding increase in the alumina content, which agrees with the findings of **(Zhang et al., 2018)**. To qualify as a suitable pozzolan for cement replacement, the sulfur trioxide (SO_3) content in raw clay should not exceed 4% **(ASTM-C-618, 2005)**, while the SO_3 content in calcined clay should remain below 1%. Remarkably, all the samples exhibit values well below 0.01%, meeting the specified criteria.

The X-ray diffraction pattern of the raw and calcined clays from Ikpeshi, Okpilla and Uzebba are presented in **Figure 5 to 7** respectively. The mineralogical composition of Ikpeshi clay is mainly kaolinite, associated with Calcite, Dollomite, Quartz and Anatase. Okpilla and Uzebba clay diffraction pattern showed the presence of two major clay minerals, that is, kaolinite and quartz. The XRD patterns of the raw clays from Ikpeshi and Uzebba showed two very high-intensity reflection peaks around 12.5 $^0 2\theta$ indicating the presence of kaolinite in the materials. The three clay samples displayed strong reflection peaks at around 27 $^0 2\theta$ indicating the presence of quartz. This is a reflection of the silica content from the XRF result (**Table 3**). The presence of Anatase, Calcite and Dollomite are indicated by high peak reflections at around 25^0, 30^0 and 31 $^0 2\theta$ respectively.

Table 3. Bulk chemical composition of the raw clays.

Material	Ikpeshi raw clay	Okpilla raw clay	Uzebba raw clay	Limestone
SiO_2 (%)	39.35	60.87	46.3	2.27
Al_2O_3 (%)	28.89	32.91	38.24	3.5
MgO (%)	0	0	0	5.9
TiO_2 (%)	4.3	2.74	5.28	1.02
Fe_2O_3 (%)	1.7	1.18	1.95	0.92
V_2O_5 (%)	0.2	0.11	0.26	0.03
CaO (%)	24.6	0.56	6.06	84.64
ZrO_2 (%)	0.15	0.41	0.53	0.03
BaO (%)	0	0.13	0.25	0
SO_3 (%)	0	0	0	0
LOI (%)	1.03	2.05	2.29	1.96
SiO_2+Al_2O_3+Fe_2O_3 (%)	70.0	95.0	86.0	7.0

The Ikpeshi and Okpilla raw clay samples showed a lower Al_2O_3 concentration (28.89 wt. % and 32.91 wt. % respectively) than the Al_2O_3 content of pure kaolinite (39.49 wt. %), while the Al_2O_3 content (38.24 wt. %) of Uzebba clay compared well with that of pure kaolinite. Also, the SiO_2 content (39.35 wt. %) of the Ikpeshi clay was lower than the SiO_2 content (46.3 wt. %) of pure kaolinite, while that of Okpilla (60.87 wt. %) is very much higher than for pure kaolinite and that of Uzebba (46.30 wt. %) is the same as that of pure kaolinite. The presence of other minerals such as dolomite and Calcite confirms the high CaO content (24.60 wt. %) in the Ikpeshi clay.

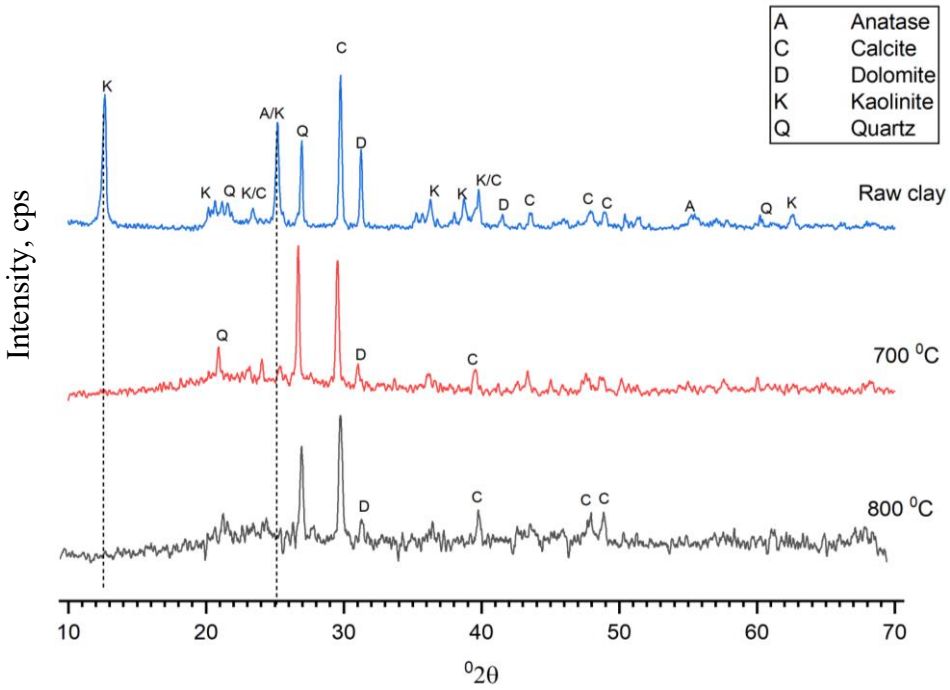

Figure 5. XRD diffraction pattern of raw and calcined clay (700 ^{0}C and 800 ^{0}C) from Ikpeshi.

Generally, it is observed from the three clay samples that at temperatures of 700 and 800 ^{0}C, the kaolinite peaks disappeared, signifying the transformation of the crystalline mineral to metakaolin, which is amorphous. However, other minerals present such as calcite and quartz remain unaffected by the calcination processes, since their decomposition temperatures are much higher than that adopted in the calcination process.

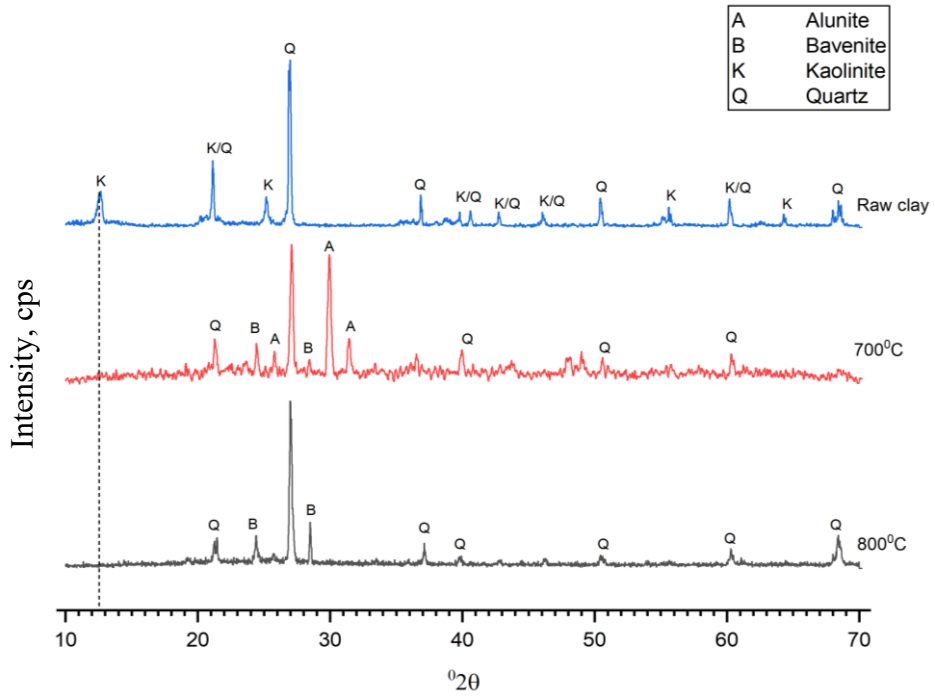

Figure 6. XRD diffraction pattern of raw and calcined clay (700 ^{0}C and 800 ^{0}C) from Okpilla.

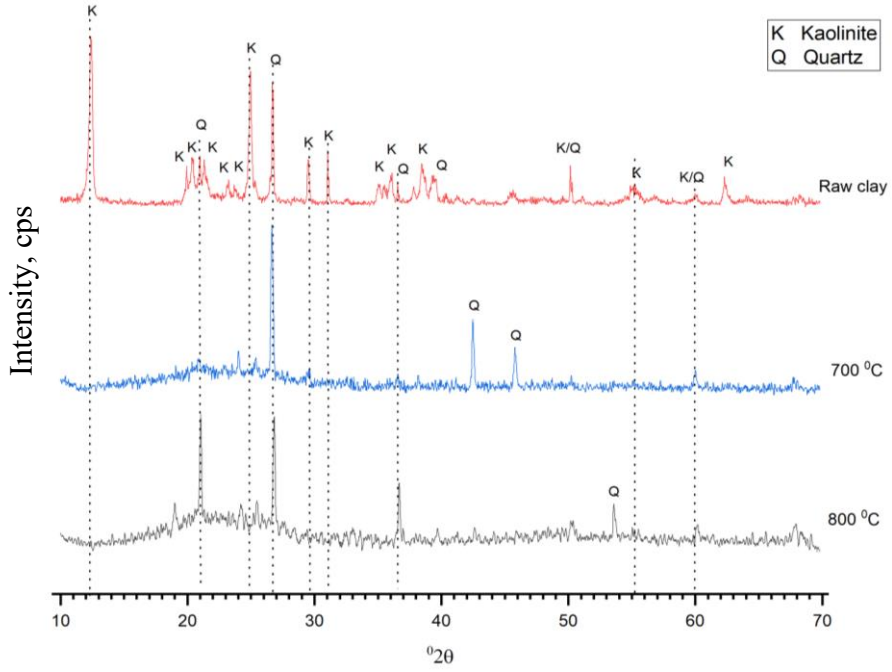

Figure 7. XRD diffraction pattern of raw and calcined clay (700 ^{0}C and 800 ^{0}C) from Uzebba.

3.2 Strength Development of Mortar Samples

The compressive strength of the mortar samples prepared from the various limestone-calcined clay blends was determined after 3, 7 and 28 days of curing. The average compressive strength of each set of test is presented in **Figure 8Error! Reference source not found.Error! Reference source not found.**

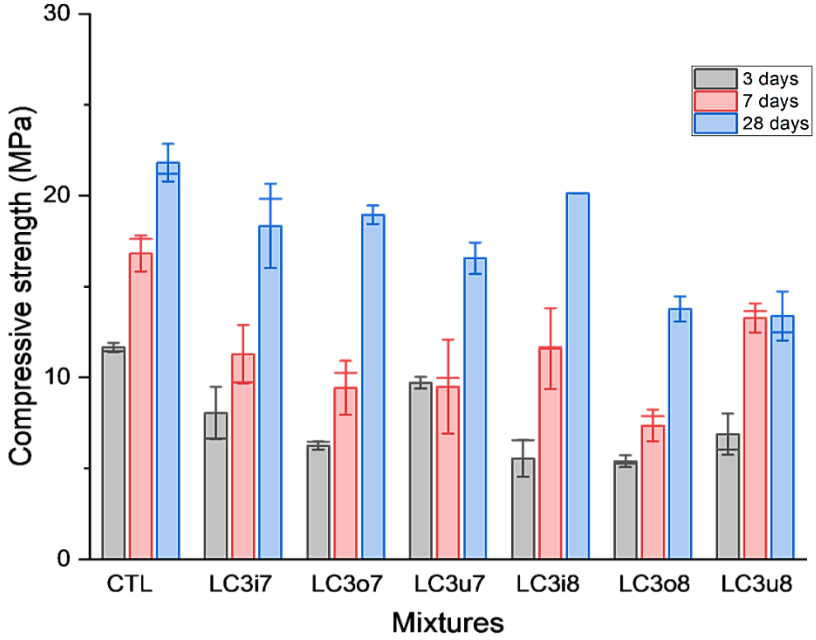

Figure 8. Compressive strength of referenced OPC (CTL) and LC3 blends from various sources (i- Ikpeshi, o- Okpilla and u- Uzebba) at clay calcination temperatures of 700 and 800 ^{0}C.

Generally, the compressive strength of all cement blends at day 3 is inferior to that of the reference sample, resulting in an activity index below unity. This discrepancy poses a significant limitation when contemplating field applications. The underlying cause can be attributed to two factors: first, the dilution effect arising from the substitution of calcined clay for lime within the cement matrix; and second, the delayed onset of the pozzolanic reaction **(Alujas et al., 2015; Shah et al., 2018; Xu et al., 2023)**. The initial reaction involves the cement hydration resulting in the formation of portlandite. It is thereafter that the calcined clay can react with the portlandite to initiate the pozzolanic reaction **(Alujas et al., 2015)**. In summary, the pozzolanic reaction of calcined kaolinites significantly contributes to strength development, particularly during the period between 7 and 28 days. Consequently, the strength values at 28 days hold greater significance for assessing the actual strength of ternary cement blends.

The compressive strength of the mortar decreases with increasing calcination temperature except for clay obtained from Ikpeshi, which displayed an increased strength upon increment in calcination temperature. The maximum compressive strength at 28 days (21.8 N/mm^2) was observed in the referenced OPC mix and the minimum value, 13.4 N/mm^2, was displayed by Uzebba calcined clay blend at 800 ^0C calcination temperature. Also there was a progressive strength development from 3 days to 28 days for all the mortar samples except for Uzebba clay blend calcined at 800 ^0C, which shows no continuous strength gain after 7 days. The limestone-calcined clay blends from Okpilla and Uzebba (at calcination temperature of 800 ^0C) displayed the lowest strength development, while the mortars blend with calcined clay from Ikpeshi (at 700 and 800 ^0C), and Okpilla (at 700 ^0C), exhibited the highest strength development relative to the referenced OPC samples. At a calcination temperature of 700°C, all calcined clay samples from Ikpeshi and Okpilla—except Uzebba—demonstrate their highest reactivity in mortars. These samples achieve a 28-day strength comparable to the reference mortar. Notably, at this temperature, these clays exhibit sufficient reactivity to function effectively as pozzolanic additives for cement and concrete. Following the results of the compressive strength of the various cement blends, calcined clay cement blend at a calcination temperature of 800 ^0C from Ikpeshi can be classified as Type B **(NF P 18-513, 2012)** having a Strength Activity Index (SAI) of 0.92, while others have a SAI ranging from 0.61 – 0.87 (**Table 4**).

Table 4. Strength activity index (SAI) of mortar samples

Sample Mix	LC3i7	LC3i8	LC3o7	LC3o8	LC3u7	LC3u8
SAI	0.84	0.92	0.87	0.63	0.65	0.61

3.3 Limestone Calcined Clay Portland Cement System

In the hardened cement paste, an assemblage of various reaction products contributes to its composition **(Lavagna and Nisticò, 2023)**. **Figure 9** illustrates the X-ray diffraction (XRD) pattern of pastes cured for 28 days, comprising pure Portland cement (PC) and LC3 blends with clays calcined at temperatures of 700°C and 800°C. The results reveal the presence of typical hydration phases, including portlandite, calcium-silicate-hydrate (C-S-H), and Strätlingite. Additionally, the blended pastes exhibit the formation of ettringite and alumina-ferric oxide trisulfate (AFt) phases.

Notably, portlandite appears crystalline, characterized by relatively intense peaks at 18.12° and 34.24° 2θ, while calcium silicate hydrate exhibits a microcrystalline structure and

appears amorphous to X-rays **(Richardson, 2008; Taylor, 1997)**. At 28 days, the amount of portlandite in the various LC3 blends was clearly reduced compared to that in the OPC paste, a similar result was obtained by **(Shah et al., 2018)**. This signifies the absorption by the alumina phase in the pozzolan to produce other hydrated phases.

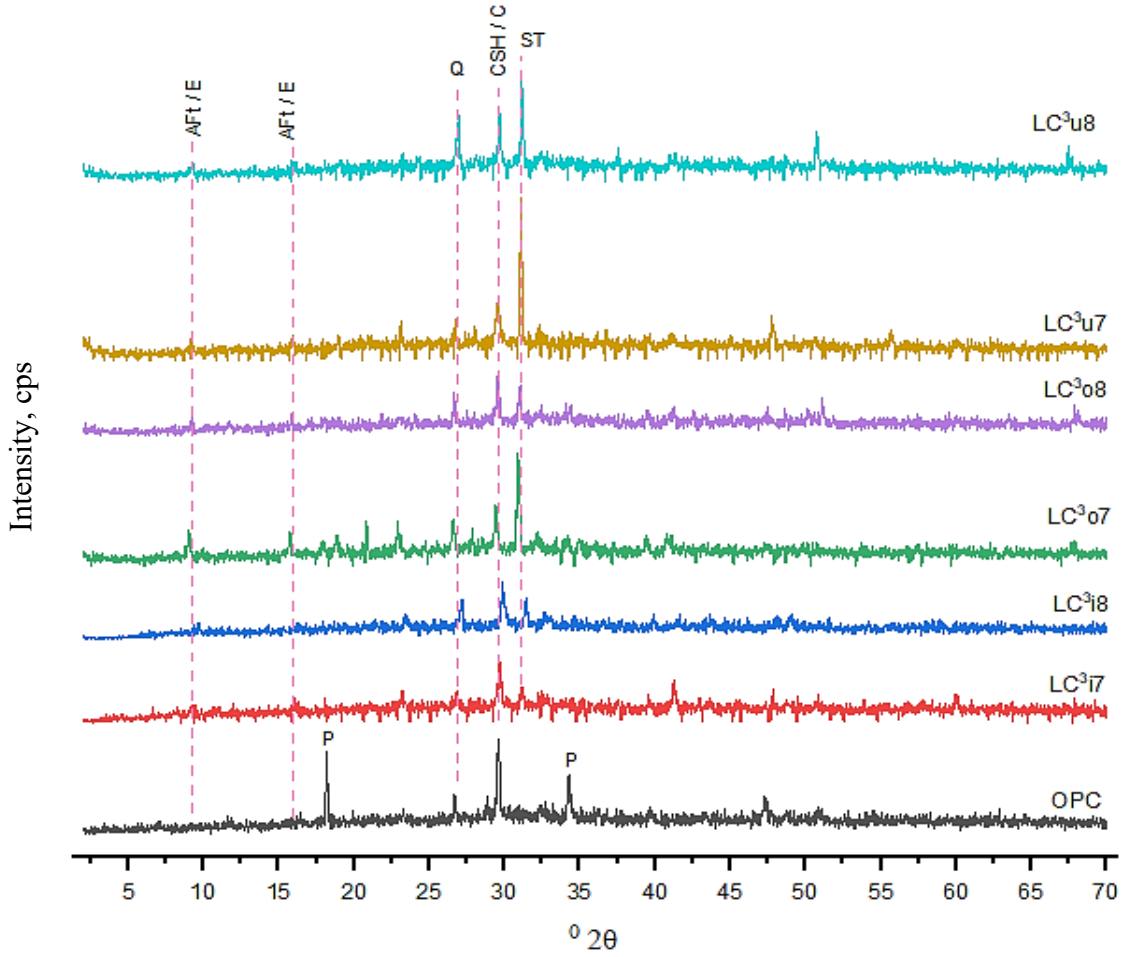

Figure 9. XRD pattern of pastes cured for 28 days of the pure OPC and of LC3 (limestone, clay calcined at 700°C and 800°C and blended with OPC). The phases that are present are indicated; P: Portlandite, St: Strätlingite, AFt: Alumina-ferric oxide trisulfate, C: Calcite, CSH: Calcium silicate hydrate, E: Ettringite, Q: Quartz.

More alumina will provoke the precipitation of strätlingite (**Cuesta et al., 2015; Singh, 2023)**, with peaks developed at around 31.18 ^{0}2θ. Strätlingite formation is evident even at 7 days, although the reflected peaks exhibit relative weakness, suggesting a low strätlingite content. However, by the 28-day mark, the peaks have significantly intensified, indicating a more pronounced contribution from the pozzolanic reaction. Interestingly, in the OPC paste, no signs of strätlingite formation were observed at 28 days. The aluminate phase reacts with water and gypsum to produce ettringite. The aluminum in ettringite and monosulfate can be partially substituted by iron (Fe) **(Möschner et al., 2009)**. The AFt phases (alumina-ferric oxide trisulfate) derived from pure ettringite with partial substitution of Al by Fe, and SO_4^{2-} by other ions are observed in all the LC3 blends with weak reflected peaks around 9.18 ^{0}2θ and 16.18 ^{0}2θ. Other observed minerals in the samples include quartz and calcite with 26.68 ^{0}2θ and 29.7 ^{0}2θ respectively.

3.4 Sorptivity

Table 5 shows the sorptivity result of the 28 days of curing samples of plain mortar and LC3 blends at the two calcination temperatures (700 ^{0}C and 800 ^{0}C). Generally, it was observed that the gradients of sorptivity tend to decrease with the replacement of the calcined clay. The sorptivity values of the LC3 mortar samples were approximately 11% to 50% lower than that of the plain mortar samples at 28 days under the same curing conditions. LC3 samples made from Ikpeshi clay at a calcination temperature of 700 ^{0}C yielded the lowest sorptivity value of 1.37 $\times 10^{-2}$ cm^3/cm^2 s$^{1/2}$, while the closest value to the referenced mortar samples (2.75 $\times 10^{-2}$ cm^3/cm^2 s$^{1/2}$) was detected in Okpilla clay (2.45 $\times 10^{-2}$ cm^3/cm^2 s$^{1/2}$) calcined at 800 ^{0}C. This is clearly reflected in the strength value developed at 28 days. The sorptivity values decrease at increasing calcination temperature for the LC3 blends from Okpilla and it decrease with a drop in calcination temperature for the Uzebba clays, these agree with their strength performance. However, LC3 samples from Ikpeshi showed a slight increase in sorptivity value from 700 to 800 ^{0}C, though there was an increase in strength moving from the lower to the higher calcination temperature.

The addition of calcined clay into the matrix improves the bond between the cement paste and the aggregate particles, resulting in improved compressive strength of the mortar samples **(Bright Singh and Murugan, 2022; Güneyisi and Mermerdaş, 2007)**. The result of the test is consistent with the report from other studies **(Boakye et al., 2024; Güneyisi and Mermerdaş, 2007)**, which confirms the superiority of limestone calcined clay cement in resisting capillary water absorption over conventional OPC.

Table 5. Variation in sorptivity of OPC and LC3 blends at different calcination temperatures

Sample ID	Temperature (^{o}C)	Sorptivity, k, (cm^3/cm^2 s$^{1/2}$) $\times 10^{-2}$
CTL	-	2.75
LC3i7	800	1.95
LC3o8		2.45
LC3u8		1.69
LC3i7	700	1.37
LC3o7		2.25
LC3u7		2.40

3.5 Resistance to Chloride Ion Penetration

Figure 10 demonstrates the chloride penetration depth measured periodically (14, 28, 56, 90 and 180 days) through the plain and LC3 mortar samples subjected to an initial curing period of 28 days in water in a fog condition, followed by immersion in salt solution. From the result, depths of chloride penetration for the referenced mortar were in the range of 7 – 19 mm depending on the immersion period in salt water. However, the LC3 mortar samples had comparatively lower chloride penetration depths, which range from 4 – 16 mm. This result agrees well with the findings by **(Ding and Li, 2002)**. They demonstrated that the integration of metakaolin-based pozollans in concrete reduced the chloride diffusion rate significantly. The maximum and minimum penetration depths of 19 mm and 8 mm at 180 days were exhibited by the referenced mortar samples and LC3 samples from Ikpeshi origin (LC3i8, i.e., clay calcined at 800 ^{0}C) respectively. The lowest free chloride penetration at age 28 days is reflected in blends from Ikpeshi (LC3i8, heated at 800 ^{0}C) and Uzebba

(LC3u8, heated at 800 ^{0}C), and the higher penetration samples are that of Okpilla (LC3o8, heated at 800 ^{0}C) and Uzebba (LC3u7, heated at 700 ^{0}C). Generally, there seems to be a reduction in the penetration depth as the calcination temperature increases from 700 to 800 ^{0}C for all blended samples. Also, the rate of penetration seems to reduce beyond 90 days of immersion for all the samples.

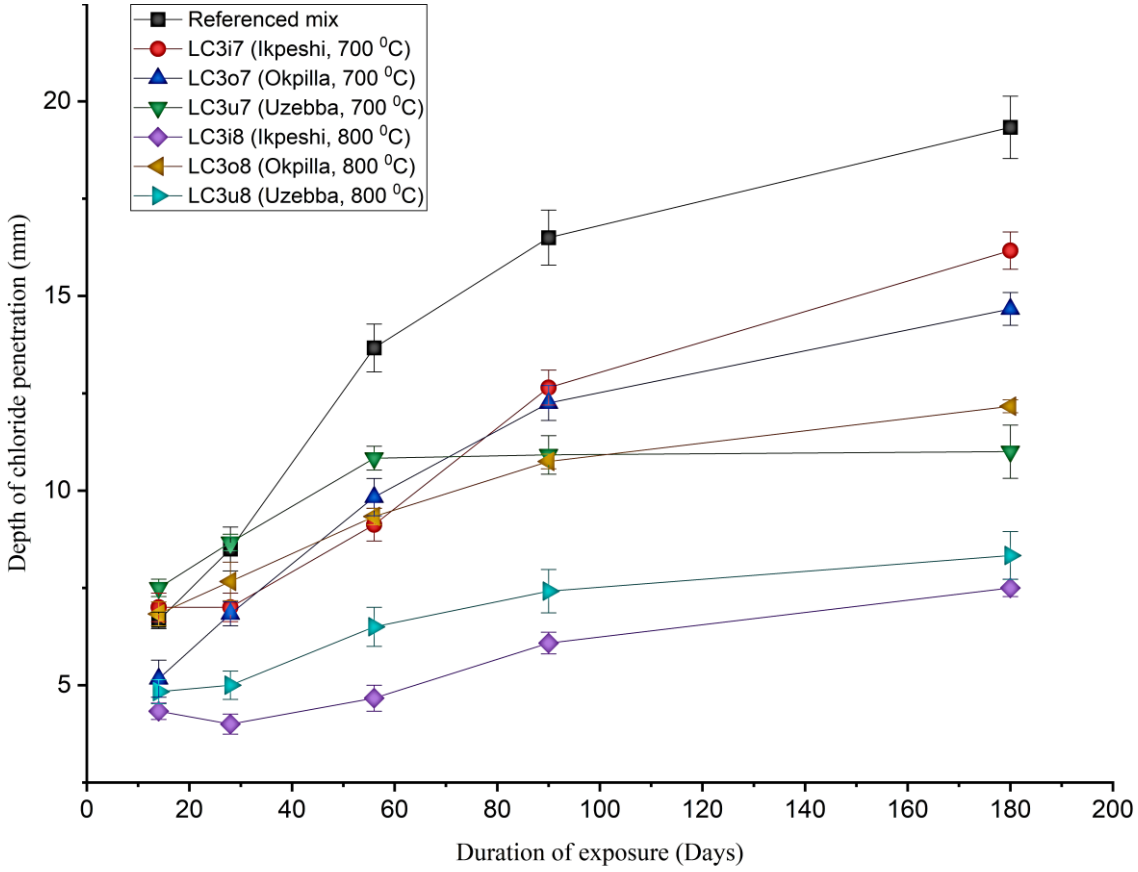

Figure 10. Variation of depth of chloride penetration with duration of exposure for plain and LC3 mortar.

4. CONCLUSIONS

The research evaluated the use of calcined clays from Nigerian deposits as supplementary materials in cement production. Key findings include:

- Calcined clays meet the criteria for pozzolans, with SiO_2, Al_2O_3, and Fe_2O_3 contents over 70%. Calcination transforms kaolinite into metakaolin, enhancing pozzolanic potential.
- The ternary cement blends showed improved strength over time, particularly between 7 and 28 days, due to pozzolanic reactions. However, initial strength at 3 days was lower than pure Portland cement.
- XRD analysis indicated typical hydration products and a reduction in portlandite, which contributed to the formation of other beneficial phases.

- Calcined clay blends generally showed lower sorptivity and reduced chloride penetration compared to standard cement, with performance varying based on calcination temperature and clay source.

Overall, calcined clays from Nigeria, particularly from Ikpeshi, show promise for sustainable cement production, helping to meet concrete demands while minimizing environmental impact.

Credit Authorship Contribution Statement

Samuel Adesina Adegbemileke: Investigation, Formal analysis, Writing – original draft. Sylvester Obinna Osuji: Supervision. Okiemute Roland Ogirigbo: Supervision, Writing – review & editing.

Declaration of Competing Interest

The authors declare that they have no known competing financial interests or personal relationships that could have appeared to influence the work reported in this paper.

REFERENCES

ACI 232.1R., 2012. Report on the Use of Raw or Processed Natural Pozzolans in Concrete.

Ademila, O., Okpoli, C., and Ehinmitan, D., 2019. Geological and lithological mapping of part of igarra schist belt using integrated geophysical methods. *Earth Sciences Pakistan*, 3, pp. 1–9. https://doi.org/10.26480/esp.01.2019.01.09

Adewumi, A. J., Omoge, O. M., and Apeabu, N., 2016. Hydrochemical assessment of groundwater for domestic and irrigation usage in Uzebba Area. *Edo State, Southwestern Nigeria*, 1(2), pp. 23–36.

Alujas, A., Fernández, R., Quintana, R., Scrivener, K. L., and Martirena, F., 2015. Pozzolanic reactivity of low grade kaolinitic clays: Influence of calcination temperature and impact of calcination products on OPC hydration. *Applied Clay Science*, 108, pp. 94–101. https://doi.org/10.1016/j.clay.2015.01.028

Arya, C., Buenfeld, N. R., and Newman, J. B., 1990. Factors influencing chloride-binding in concrete. Cement and Concrete Research, 20(2), pp. 291–300. https://doi.org/10.1016/0008-8846(90)90083-A

Arya, C., and Xu, Y., 1995. Effect of cement type on chloride binding and corrosion of steel in concrete. *Cement and Concrete Research*, 25(4), pp. 893–902. https://doi.org/10.1016/0008-8846(95)00080-V

ASTM-C109/109M., 2008. Standard test method for compressive strength of hydraulic cement mortars (Using 2-in. or cube specimens). In Annual Book of ASTM Standards.

ASTM-C-618., 2005. Standard Specification for Coal Fly Ash and Raw or Calcined Natural Pozzolan for Use. ASTM International.

ASTM C1585., 2009. Standard Test Method for Measurement of Rate of Absorption of Water by Hydraulic- Cement Concretes. ASTM International. 1–6.

ASTM-C1602/C1602M., 2012. Standard Specification for Mixing Water Used in the Production of Hydraulic Cement Concrete. ASTM Lnternational.

ASTM C 778., 2002. Standard Specification for Standard Sand (Vol. 14). https://doi.org/10.1520/C0778-21

Avet, F., Snellings, R., Alujas, D. A., Ben, H. M., and Scrivener, K., 2016. Development of a new rapid, relevant and reliable (R3) test method to evaluate the pozzolanic reactivity of calcined kaolinitic clays. *Cement and Concrete Research*, 85, pp. 1–11. https://doi.org/10.1016/J.CEMCONRES.2016.02.015

Bai, J., Wild, S., and Sabir, B. B., 2002. Sorptivity and strength of air-cured and water-cured PC–PFA–MK concrete and the influence of binder composition on carbonation depth. Cement and Concrete Research, 32(11), pp. 1813–1821. https://doi.org/10.1016/S0008-8846(02)00872-4

Balakrishna, M., Mohamad, F., Evans, R., and Rahman, M., 2018. Assessment of sorptivity coefficient in concrete cubes. *Discovery,* 54(274), pp. 377–386.

Boakye, K., Khorami, M., Saidani, M., Ganjian, E., Tyrer, M., and Dunster, A., 2024. Performance of a single source of low-grade clay in a limestone calcined clay cement mortar. *Buildings*, 14(1). https://doi.org/10.3390/buildings14010093

Bright Singh, S., and Murugan, M., 2022. Effect of metakaolin on the properties of pervious concrete. *Construction and Building Materials*, 346(128476). https://doi.org/10.1016/j.conbuildmat.2022.128476

BS EN 196-1., 1995. Methods of testing cement — Part 1: Determination of strength.

Cuesta, A., De la Torre, A., Santacruz, I., Cabeza, A., Alvarez-Pinazo, G., Aranda, M., and Sanz, J., 2015. Structure of stratlingite and effect of hydration methodology on microstructure. *Advances in Cement Research*, 28, pp. 1–10. https://doi.org/10.1680/adcr.14.00104

Díaz, Y. C., Berriel, S. S., Heierli, U., Favier, A. R., Machado, I. R. S., Scrivener, K. L., and Habert, G., 2017. Limestone calcined clay cement as a low-carbon solution to meet expanding cement demand in emerging economies. *Development Engineering*, 2(June), pp. 82–91. https://doi.org/10.1016/j.deveng.2017.06.001

Ding, J.T., and Li, Z. J., 2002. Effects of metakaolin and silica fume on properties of concrete. *ACI Materials Journal*, 99, pp. 393–398.

Güneyisi, E., and Gesoğlu, M., 2008. A study on durability properties of high-performance concretes incorporating high replacement levels of slag. *Materials and Structures*, 41(3), 479–493. https://doi.org/10.1617/s11527-007-9260-y

Güneyisi, E., and Mermerdaş, K., 2007. Comparative study on strength, sorptivity, and chloride ingress characteristics of air-cured and water-cured concretes modified with metakaolin. *Materials and Structures/Materiaux et Constructions*, 40(10), pp. 1161–1171. https://doi.org/10.1617/s11527-007-9258-5

Güneyisi, E., Ozturan, T., and Gesog˘lu, M., 2007. Effect of initial curing on chloride ingress and corrosion resistance characteristics of concretes made with plain and blended cements. *Building and Environment*, 42. https://doi.org/10.1016/j.buildenv.2006.07.008

Hedayat, A. A., and Baniasadizade, M., 2015. Evaluation of the different test methods of the concrete durability for the Persian Gulf Environment. *Advances in Structural Engineering*, 18(10), pp. 1575–1586. https://doi.org/10.1260/1369-4332.18.10.1575

Juenger, M. C. G., Snellings, R., and Bernal, S. A., 2019. Supplementary cementitious materials: New sources, characterization, and performance insights. *Cement and Concrete Research*, 122, pp. 257–273. https://doi.org/10.1016/j.cemconres.2019.05.008

Kim, M., Yang, E., and Yi, S., 2007. Evaluation of chloride penetration characteristics using a colorimetric method in concrete structures, *Engineering, Materials Science*, pp. 1–6.

Lavagna, L., and Nisticò, R., 2023. An Insight into the Chemistry of Cement—A Review. *Applied Sciences*, 13(1). https://doi.org/10.3390/app13010203

Loser, R., Lothenbach, B., Leemann, A., and Tuchschmid, M., 2010. Chloride resistance of concrete and its binding capacity – Comparison between experimental results and thermodynamic modeling. *Cement and Concrete Composites*, 32(1), pp. 34–42. https://doi.org/10.1016/J.CEMCONCOMP.2009.08.001

Luping, T., and Nilsson, L.-O., 1993. Chloride binding capacity and binding isotherms of OPC pastes and mortars. *Cement and Concrete Research*, 23. https://doi.org/10.1016/0008-8846(93)90089-R

Möschner, G., Lothenbach, B., Winnefeld, F., Ulrich, A., Figi, R., and Kretzschmar, R., 2009. Solid solution between Al-ettringite and Fe-ettringite (Ca6[Al1−xFex(OH)6]2(SO4)3·26H2O). *Cement and Concrete Research*, 39(6), pp. 482–489. https://doi.org/10.1016/J.CEMCONRES.2009.03.001

NF P18-513., 2012. Métakaolin, addition pouzzolanique pour bétons: définitions, spécification, citères de conformité.

Odriozola, B.M.Á., and Gutiérrez, A.P., 2008. Comparative study of different test methods for reinforced concrete durability assessment in marine environment. *Materials and Structures*, 41(3), pp. 527–541. https://doi.org/10.1617/s11527-007-9263-8

Ogirigbo, O. R., and Black, L., 2017. Chloride binding and diffusion in slag blends: Influence of slag composition and temperature. *Construction and Building Materials*, 149(3), pp. 816–825. https://doi.org/10.1016/j.conbuildmat.2017.05.184

Ogirigbo, O.R., 2016. Influence of slag composition and temperature on the hydration and performance of slag blends in chloride environments (Doctoral dissertation, University of Leeds).

Rautureau, M., Gomes, C. de S.F., Liewig, N., and Katouzian-Safadi, M., 2017. Clays and health: Properties and therapeutic uses. *Clays and Health: Properties and Therapeutic Uses*, pp. 1–217. https://doi.org/10.1007/978-3-319-42884-0

Richardson, I. G., 2008. The calcium silicate hydrates. *Cement and Concrete Research*, 38(2), pp. 137–158. https://doi.org/10.1016/J.CEMCONRES.2007.11.005

Sabir, B., Wild, S., and Bai, J., 2001. Metakaolin and calcined clays as pozzolans for concrete: A review. *Cement and Concrete Composites*, 23(6), pp. 441–454. https://doi.org/10.1016/S0958-9465(00)00092-5

Scrivener, K. L., 2014. Options for the future of cement. The Indian Concrete Journal, 88(7), 11–21.

Shah, V., Parashar, A., Mishra, G., Medepalli, S., Krishnan, S., and Bishnoi, S., 2018. Influence of cement replacement by limestone calcined clay pozzolan on the engineering properties of mortar and concrete. *Advances in Cement Research*, pp. 1–11. https://doi.org/10.1680/jadcr.18.00073

Singh, V. K., 2023. Classification of pozzolana and production of pozzolanic cements. *The Science and Technology of Cement and Other Hydraulic Binders*, pp. 653–694. https://doi.org/10.1016/B978-0-323-95080-0.00018-2

Stark, J., and Wicht, B., 2000. Einführung. In Zement und Kalk. *Basel: Birkhäuser Basel*. https://doi.org/10.1007/978-3-0348-8382-5_1

Tasdemir, C., 2003. Combined effects of mineral admixtures and curing conditions on the sorptivity coefficient of concrete. *Cement and Concrete Research*, 33(10), pp. 1637–1642. https://doi.org/10.1016/S0008-8846(03)00112-1

Taylor, H. F., 1997. Cement chemistry (2nd ed.). Thomas Telford Publishing.

Xu, X., Zhao, Y., Gu, X., Zhu, Z., Wang, F., and Zhang, Z., 2023. Effect of particle size and morphology of siliceous supplementary cementitious material on the hydration and autogenous shrinkage of blended cement. *Materials*, 16(4). https://doi.org/10.3390/ma16041638

Zhang, R., Gong, E., Wang, G., and Yang, Z., 2018. An analytical shortcut to estimate alumina content by LOI in Lateritic Gibbsite Bauxite Prospecting. In 11th Alumina Quality Workshop International Conference (pp. 1–5). Gladstone, Queensland, Australia.

استكشاف إمكانات البوزولان النيجيري المبني على الطين لتعزيز أداء الخرسانة واستدامتها: دراسة عن القوة والترطيب والمتانة

صامويل أديسينا أديجبيميليكي*، سيلفستر أوبينا أوسوجي، أوكيموت رولاند أوجيريجبو

قسم الهندسة المدنية، جامعة بنين، مدينة بنين، نيجيريا

الخلاصة

حثت هذه الدراسة في إمكانية استخدام الطين المكلس من الرواسب النيجيرية في إنتاج خلطات ثلاثية من الأسمنت. تم الحصول على عينات الطين من ثلاثة مواقع مختلفة وهي: إكبيشي، أوكبيلا، وأوزيبا. تم بعد ذلك تحميص عينات الطين الخام عند 700 درجة مئوية و800 درجة مئوية. تم تحديد التركيب الكيميائي والمعدني لعينات الطين الخام والمكلس باستخدام XRF وXRD على التوالي. أكد التركيب الكيميائي أن هذه الطينات هي بوزولانات محتملة مع SiO_2، Al_2O_3، وFe_2O_3 مجتمعة تتجاوز 70٪. وقد حدد تحليل XRD الكاولينيت والكوارتز كمراحل معدنية رئيسية في الطين الخام، والتي تتحول إلى ميتاكاولين عند التكليس. أظهرت اختبارات قوة الضغط على عينات الملاط المحضرة باستبدال 50% من الأسمنت البورتلاندي بالطين المكلس والحجر الجيري، أن طين الإكبيشي عند 800 درجة مئوية يتمتع بأفضل أداء للقوة، مع مؤشر نشاط قوة يبلغ 0.92 عند 28 يومًا، مما يدل على إمكانات بوزولانية متفوقة. كان تطور القوة أكثر أهمية بين 7 و28 يومًا، مما يشير إلى مساهمة التفاعل البوزولاني في القوة على المدى الطويل. ومع ذلك، كانت القوة الأولية عند 3 أيام أقل من الأسمنت المرجعي بسبب تأخر تفاعل البوزولان. كشف تحليل XRD للمعاجين المخلوطة عن مراحل ترطيب نموذجية مثل البورتلانديت، و$C-S-H$، والستراتلينجيت، والإترينجيت، مع إظهار الخلطات الثلاثية انخفاض محتوى البورتلانديت، مما يشير إلى الامتصاص بواسطة مرحلة ألومينا البوزولان. كشفت تقييمات المتانة أن الخلطات الثلاثية أظهرت مقاومة محسنة لدخول أيونات الماء والكلوريد. تسلط هذه النتائج الضوء على فعالية الطين النيجيري المكلس في إنتاج خرسانة متينة ومستدامة، ودعم استخدامها كمواد أسمنتية تكميلية لتقليل التأثير البيئي لإنتاج الخرسانة.

الكلمات المفتاحية: الطين المكلس، الحجر الجيري، المواد الأسمنتية التكميلية، الأسمنت البورتلاندي، الطين النيجيري.